Detecting Sensor Failure via Decoupled Error Function and Inverse Input–Output Model

Zhiling Li[1]; B. H. Koh[2]; and Satish Nagarajaiah[3]

Abstract: A novel sensor failure detection method is developed in this paper. Sensor failure considered in this paper can be any type of measurement error that is different from the true structural response. The sensors are divided into two groups; sensors that correctly measure the structural responses are termed "reference sensors" and sensors that may fail to correctly measure the structural responses are termed "uncertain sensors" henceforth. A sensor error function is formulated to detect the instants of failure of the corresponding uncertain sensor, using the measurements from reference sensors and the uncertain sensor examined. The sensor error function is derived using indirect and direct approaches. In the indirect approach, the error function is obtained from the state space model in combination with the inverse model and interaction matrix formulation. The input term is eliminated from the error function by applying the inverse model and the interaction matrix is applied to eliminate the state and all unexamined uncertain sensors except for the one examined from the error function. The direct approach uses the singular value decomposition method to establish the coefficients of the error function from the healthy measured data. The sensor failure detection formulation is investigated numerically using a four degree-of-freedom spring-mass-damper system and experimentally using a 4-m-long NASA eight-bay truss structure. It is shown by means of numerical and experimental results that the sensor failure formulation developed correctly detects and isolates the instants of sensor failure and can be implemented in real structural systems for sensor failure detection.

DOI: 10.1061/(ASCE)0733-9399(2007)133:11(1222)

CE Database subject headings: Sensors; Failures; Errors; Structural response.

Introduction

Sensor failure is defined as the measurement that is different from the true response of the structure. It is very important to detect sensor failure on a real-time basis for vibration control and structural health monitoring. Various fault detection and isolation (FDI) techniques for sensors and actuators have been discussed over the past decades (Frank 1990, Gertler 1991). The two major sensor failure detection methods are approaches that exploit: (1) physical redundancy; and (2) analytical redundancy. Physical redundancy uses more than one physical sensor to measure the responses from the same degree of freedom. The analytical redundancy (AR) method, which implies the inherent redundancy contained in the static and dynamic relationship among the system inputs and measured outputs, has been applied broadly both in adaptive control and fault tolerant systems. The method developed in this study belongs to one of the AR-based methods.

Most of the sensor failure detection methods relying on AR strategy (Park et al. 1993; Da and Lin 1995; Chen and Speyer 2001; Piercy 1992; Menke 1995; Dharap et al. 2006) can be traced back to Beard-Jones detection filters (BJDT) (Beard 1971; Jones 1976), which assign fixed directional properties to the error function through observers' design. There are two mains steps in BJDT. First, an error function corresponding to one actuator/sensor/component is developed, which is zero or near zero when there is no error and is different from zero when the corresponding actuator/sensor/component fails. Then a decision rule is applied to determine whether errors occur or not. In BJDT, sensor failure is normally treated as actuator failure, which is termed "pseudoactuator failure," and normally can only be constrained to lie in a geometric plane. Park et al. (1993) have provided an algorithm that can isolate each sensor failure in a fixed direction in output space by augmenting the number of states to account for the dynamics of the sensor failure.

Phan and coworkers (Phan et al. 1998; Lim et al. 1998; Goodzeit and Phan 2000) have shown that the interaction matrix can be applied to eliminate state variables so that only input and output are needed to represent the system's dynamics. Koh et al. (2005a,b) have applied the concept of interaction matrix to build actuator error function, which eliminates the influence of other actuators from the actuator error function except for the examined one. The actuator error function will be nonzero when the examined actuator fails. Kammer and co-workers (Kammer 1997; Kammer and Steltzner 2001) have applied an inverse model to estimate the remote sensor responses and estimate the input forces from the structural responses. To estimate the remote sensor responses (Kammer 1997), the input terms are first eliminated from

[1]Postdoctoral Research Associate, Dept. of Civil and Environmental Engineering, Rice Univ., Houston, TX 77005; Formerly, Graduate Student.

[2]Assistant Professor, Dept. of Mechanical Engineering, Dongguk Univ., Seoul 100-715, Republic of Korea

[3]Professor, Dept. of Civil and Environmental Engineering, and Dept. of Mechanical Engineering and Material Science, Rice Univ., Houston, TX 77005 (Corresponding author). E-mail: nagaraja@rice.edu

Note. Associate Editor: Raimondo Betti. Discussion open until April 1, 2008. Separate discussions must be submitted for individual papers. To extend the closing date by one month, a written request must be filed with the ASCE Managing Editor. The manuscript for this paper was submitted for review and possible publication on December 22, 2004; approved on November 14, 2005. This paper is part of the ***Journal of Engineering Mechanics***, Vol. 133, No. 11, November 1, 2007. ©ASCE, ISSN 0733-9399/2007/11-1222–1228/$25.00.

the state-space model by introducing the inverse model and only measured sensor responses and remote sensor responses are retained. Then the Markov parameters corresponding to the inverse model are obtained by a transformation matrix, which is either obtained indirectly from the state-space model or directly from measurement only.

In this paper, the concept of actuator failure detection formulation (Koh et al. 2005a,b) and inverse model (Kammer 1997; Kammer and Steltzner 2001) are combined to develop an algorithm that detects and isolates sensor failure in realtime. In this formulation, sensors are separated into two groups as needed by the inverse model technique (to be described in "Sensor Error Function Computed Indirectly Using State-Space Matel"). Sensors in the first group are assumed to correctly measure the structural responses and are termed "reference sensors" henceforth. Sensors in the second group that need to be monitored are termed "uncertain sensors" henceforth. A sensor error function is developed, one for each uncertain sensor, to monitor the instant failure of the uncertain sensor and it is not influenced by the measurement of other uncertain sensors. The sensor error function is developed in two ways. First, the sensor error function is derived from the system state-space model. The inverse model is applied to eliminate the input term from the state-space equation, and then an interaction matrix is introduced to eliminate the state variables and all uncertain sensor terms except for the examined one from the sensor error function. Then a sensor error function is derived, one for each uncertain sensor, to monitor the instant failure of the uncertain sensor examined. The error function produces a nonzero signal when the examined sensor fails to correctly measure the structural response. The necessary conditions for the sensor failure detection formulation are also discussed. Second, using the singular value decomposition method, the coefficients of the sensor error function are established in the null space of the healthy measurements from both reference sensors and the uncertain sensor examined. Both numerical and experimental results show that the sensor error functions developed can successfully detect and isolate examined uncertain sensor failure in real time.

Mathematical Formulation

Sensor Error Function Computed Indirectly Using State-Space Model

Consider an nth order, r-input, q-output controllable and observable linear time-invariant discrete model in the state-space system

$$\mathbf{x}(k+1) = \mathbf{A}\mathbf{x}(k) + \mathbf{B}\mathbf{u}(k)$$

$$\mathbf{y}(k) = \mathbf{C}\mathbf{x}(k) + \mathbf{D}\mathbf{u}(k) \tag{1}$$

in which $\mathbf{x}$ represents an n dimensional state vector; $\mathbf{A}=n\times n$ system state transmission matrix; $\mathbf{B}=n\times r$ input influence matrix; $\mathbf{u}=r$ dimensional input force vector; $\mathbf{y}=q$ dimensional output vector; $\mathbf{C}=q\times n$ output influence matrix; and $\mathbf{D}=q\times r$ direct transmission matrix.

The output in Eq. (1) can be separated into two groups: $\mathbf{y}_s(k)$ and $\mathbf{y}_d(k)$, where $\mathbf{y}_s(k)$ is the measurement from reference sensors and $\mathbf{y}_d(k)$ is the measurement from uncertain sensors. Rewrite Eq. (1) for the measurement $\mathbf{y}_d(k)$

$$\mathbf{x}(k+1) = \mathbf{A}\mathbf{x}(k) + \mathbf{B}\mathbf{u}(k)$$

$$\mathbf{y}_d(k) = \mathbf{C}_d\mathbf{x}(k) + \mathbf{D}_d\mathbf{u}(k) \tag{2}$$

where $\mathbf{y}_d(k)=n_d$ (number of uncertain sensors) dimensional vector; $\mathbf{C}_d=n_d\times n$ output influence matrix for the uncertain sensors; and $\mathbf{D}_d=n_d\times r$ direct transmission matrix from input to the uncertain sensors. The direct transmission matrix $\mathbf{D}_d$ is assumed to be full row rank here. For the case where $\mathbf{D}_d$ is not full column rank, the method proposed by Steltzner and Kammer (1999) can be adopted. Solving the output $\mathbf{y}_d(k)$ in Eq. (2) for input $\mathbf{u}(k)$

$$\mathbf{u}(k) = -\mathbf{D}_d^{+}\mathbf{C}_d\mathbf{x}(k) + \mathbf{D}_d^{+}\mathbf{y}_d(k) \tag{3}$$

where $\mathbf{D}_d^{+}$=pseudoinverse of $\mathbf{D}_d$ and $\mathbf{D}_d^{+}=(\mathbf{D}_d^T\mathbf{D}_d)^{-1}\mathbf{D}_d^T$. In order for the pseudoinverse to uniquely exist, the number of uncertain sensors n_d must be larger than or equal to the number of inputs r. Substituting Eq. (3) into the state equation in Eq. (2) produces

$$\mathbf{x}(k+1) = (\mathbf{A} - \mathbf{B}\mathbf{D}_d^{+}\mathbf{C}_d)\mathbf{x}(k) + \mathbf{B}\mathbf{D}_d^{+}\mathbf{y}_d(k) \tag{4}$$

By defining: $\bar{\mathbf{A}}=\mathbf{A}-\mathbf{B}\mathbf{D}_d^{+}\mathbf{C}_d$, $\bar{\mathbf{B}}=\mathbf{B}\mathbf{D}_d^{+}$, $\bar{\mathbf{C}}_d=-\mathbf{D}_d^{+}\mathbf{C}$, $\bar{\mathbf{D}}_d=\mathbf{D}_d^{+}$, Eqs. (3) and (4) can be rewritten as

$$\mathbf{x}(k+1) = \bar{\mathbf{A}}\mathbf{x}(k) + \bar{\mathbf{B}}\mathbf{y}_d(k)$$

$$\mathbf{u}(k) = \bar{\mathbf{C}}_d\mathbf{x}(k) + \bar{\mathbf{D}}_d\mathbf{y}_d(k) \tag{5}$$

The inputs and outputs shown in Eq. (5) have been switched, which is an inverse model of Eq. (2). The state and output equations between the input and output of reference sensors can be expressed as

$$\mathbf{x}(k+1) = \mathbf{A}\mathbf{x}(k) + \mathbf{B}\mathbf{u}(k)$$

$$\mathbf{y}_s(k) = \mathbf{C}_s\mathbf{x}(k) + \mathbf{D}_s\mathbf{u}(k) \tag{6}$$

$\mathbf{y}_s(k)=n_s$ (number of reference sensors) dimensional measurement vector; $\mathbf{C}_s=n_s\times n$ output influence matrix for reference sensors; and $\mathbf{D}_s=n_s\times r$ direct transmission matrix from input to the reference sensors. Substituting Eq. (3) into Eq. (6) produces

$$\mathbf{x}(k+1) = \bar{\mathbf{A}}\mathbf{x}(k) + \bar{\mathbf{B}}\mathbf{y}_d(k) \tag{7}$$

$$\mathbf{y}_s(k) = (\mathbf{C}_s - \mathbf{D}_s\mathbf{D}_d^{+}\mathbf{C}_d)\mathbf{x}(k) + \mathbf{D}_s\mathbf{D}_d^{+}\mathbf{y}_d(k)$$

Defining $\bar{\mathbf{C}}_s=\mathbf{C}_s-\mathbf{D}_s\mathbf{D}_d^{+}\mathbf{C}_d$ and $\bar{\mathbf{D}}_s=\mathbf{D}_s\mathbf{D}_d^{+}$, Eq. (7) can be expressed as

$$\mathbf{x}(k+1) = \bar{\mathbf{A}}\mathbf{x}(k) + \bar{\mathbf{B}}\mathbf{y}_d(k)$$

$$\mathbf{y}_s(k) = \bar{\mathbf{C}}_s\mathbf{x}(k) + \bar{\mathbf{D}}_s\mathbf{y}_d(k) \tag{8}$$

Eq. (8) represents an inverse model where the measurements from uncertain sensors are treated as inputs and the measurements from the reference sensors are treated as outputs. The input terms that exert forces to the structure have been completely eliminated from the state-space equation. Assuming that sensors measure the responses of independent degree of freedoms and each sensor will not be collocated with other sensors, the $\bar{\mathbf{D}}_s$ term will be a null matrix. Eq. (8) can be rewritten as

$$\mathbf{x}(k+1) = \bar{\mathbf{A}}\mathbf{x}(k) + \bar{\mathbf{B}}\mathbf{y}_d(k)$$

$$\mathbf{y}_s(k) = \bar{\mathbf{C}}_s\mathbf{x}(k) \tag{9}$$

By repeated substitution for some $p>0$

$$\mathbf{x}(k+p) = \bar{\mathbf{A}}^p \mathbf{x}(k) + \boldsymbol{\tau} \mathbf{y}_{pd}(k)$$

$$\mathbf{y}_{ps}(k) = \mathbf{O}\mathbf{x}(k) + \mathbf{T}\mathbf{y}_{pd}(k) \tag{10}$$

where $\mathbf{y}_{\text{pd}}(k)$ and $\mathbf{y}_{\text{ps}}(k)$=column vectors of the measured data from the uncertain sensors and the reference sensors going into p steps starting with $\mathbf{y}_d(k)$ and $\mathbf{y}_s(k)$, respectively

$$\mathbf{y}_{pd}(k) = \begin{pmatrix} \mathbf{y}_d(k) \\ \mathbf{y}_d(k+1) \\ \vdots \\ \mathbf{y}_d(k+p-1) \end{pmatrix}, \quad \mathbf{y}_{ps}(k) = \begin{pmatrix} \mathbf{y}_s(k) \\ \mathbf{y}_s(k+1) \\ \vdots \\ \mathbf{y}_s(k+p-1) \end{pmatrix} \tag{11}$$

where $\boldsymbol{\tau}$=extended $n \times pn_d$ controllability matrix, $\mathbf{O}$=extended $pn_s \times n$ observability matrix; and $\mathbf{T}=pn_d \times pn_s$ "Toeplitz" matrix of the inverse system Markov parameters

$$\boldsymbol{\tau} = [\bar{\mathbf{A}}^{p-1}\bar{\mathbf{B}} \ \cdots \ \bar{\mathbf{A}}\bar{\mathbf{B}} \ \bar{\mathbf{B}}]$$

$$\mathbf{O} = \begin{bmatrix} \bar{\mathbf{C}}_s \\ \bar{\mathbf{C}}_s\bar{\mathbf{A}} \\ \vdots \\ \bar{\mathbf{C}}_s\bar{\mathbf{A}}^{p-1} \end{bmatrix}, \quad \mathbf{T} = \begin{bmatrix} \mathbf{0} & \mathbf{0} & \cdots & \mathbf{0} & \mathbf{0} \\ \bar{\mathbf{C}}_s\bar{\mathbf{B}} & \mathbf{0} & \cdots & \mathbf{0} & \mathbf{0} \\ \bar{\mathbf{C}}_s\bar{\mathbf{A}}\bar{\mathbf{B}} & \bar{\mathbf{C}}_s\bar{\mathbf{B}} & \cdots & \mathbf{0} & \mathbf{0} \\ \vdots & \ddots & \ddots & \ddots & \vdots \\ \bar{\mathbf{C}}_s\bar{\mathbf{A}}^{p-2}\bar{\mathbf{B}} & \cdots & \bar{\mathbf{C}}_s\bar{\mathbf{A}}\bar{\mathbf{B}} & \bar{\mathbf{C}}_s\bar{\mathbf{B}} & \mathbf{0} \end{bmatrix} \tag{12}$$

Rewrite Eq. (10) with each individual uncertain sensor for p steps

$$\mathbf{x}(k+p) = \bar{\mathbf{A}}^p\mathbf{x}(k) + \sum_{j=1}^{n_d} \boldsymbol{\tau}_j \mathbf{y}_{pd}^j(k) + \sum_{j=1}^{n_d} \bar{\mathbf{B}}_j \mathbf{y}_d^j(k+p-1)$$

$$\mathbf{y}_{ps}(k) = \mathbf{O}\mathbf{x}(k) + \sum_{j=1}^{n_d} \mathbf{T}_j \mathbf{y}_{pd}^j(k) \tag{13}$$

where

$$\boldsymbol{\tau}_j = [\bar{\mathbf{A}}^{p-1}\bar{\mathbf{B}}_j \ \cdots \ \bar{\mathbf{A}}^2\bar{\mathbf{B}}_j \ \bar{\mathbf{A}}\bar{\mathbf{B}}_j]$$

$$\mathbf{y}_{pd}^j(k) = \begin{pmatrix} y_{dj}(k) \\ y_{dj}(k+1) \\ \vdots \\ y_{dj}(k+p-2) \end{pmatrix}$$

$$\mathbf{T}_j = \begin{bmatrix} \mathbf{0} & \mathbf{0} & \cdots & \mathbf{0} \\ \bar{\mathbf{C}}_s\bar{\mathbf{B}}_j & \mathbf{0} & \cdots & \mathbf{0} \\ \bar{\mathbf{C}}_s\bar{\mathbf{A}}\bar{\mathbf{B}}_j & \bar{\mathbf{C}}_s\bar{\mathbf{B}}_j & \cdots & \mathbf{0} \\ \vdots & \ddots & \ddots & \cdots \\ \bar{\mathbf{C}}_s\bar{\mathbf{A}}^{\mathbf{p}-2}\bar{\mathbf{B}}_j & \cdots & \bar{\mathbf{C}}_s\bar{\mathbf{A}}\bar{\mathbf{B}}_j & \bar{\mathbf{C}}_s\bar{\mathbf{B}}_j \end{bmatrix} \tag{14}$$

An interaction matrix $\mathbf{M}_i$ is introduced by adding and subtracting the product $\mathbf{M}_i\mathbf{y}_{ps}(k)$ to Eq. (13) as follows

$$\begin{aligned} \mathbf{x}(k+p) &= \bar{\mathbf{A}}^p\mathbf{x}(k) + \sum_{j=1}^{n_d} \boldsymbol{\tau}_j \mathbf{y}_{pd}^j(k) + \mathbf{M}_i\mathbf{y}_{ps}(k) - \mathbf{M}_i\mathbf{y}_{ps}(k) \\ &\quad + \sum_{j=1}^{n_d} \bar{\mathbf{B}}_j\mathbf{y}_d^j(k+p-1) = (\bar{\mathbf{A}}^p + \mathbf{M}_i\mathbf{O})\mathbf{x}(k) \\ &\quad + \sum_{j=1}^{n_d} (\boldsymbol{\tau}_j + \mathbf{M}_i\mathbf{T}_j)\mathbf{y}_{pd}^j(k) - \mathbf{M}_i\mathbf{y}_{ps}(k) + \sum_{j=1}^{n_d} \bar{\mathbf{B}}_j\mathbf{y}_d^j(k+p-1) \end{aligned} \tag{15}$$

Substituting Eq. (15) into the output equation in Eq. (9) for the $k+p$ step

$$\begin{aligned} \mathbf{y}_s(k+p) &= (\bar{\mathbf{C}}_s\bar{\mathbf{A}}^p + \bar{\mathbf{C}}_s\mathbf{M}_i\mathbf{O})\mathbf{x}(k) + \sum_{j=1}^{n_d} (\bar{\mathbf{C}}_s\boldsymbol{\tau}_j + \bar{\mathbf{C}}_s\mathbf{M}_i\mathbf{T}_j)\mathbf{y}_{pd}^j(k) \\ &\quad - \bar{\mathbf{C}}_s\mathbf{M}_i\mathbf{y}_{ps}(k) + \sum_{j=1}^{n_d} \bar{\mathbf{C}}_s\bar{\mathbf{B}}_j\mathbf{y}_d^j(k+p-1) \end{aligned} \tag{16}$$

By imposing the constraint condition in Eq. (17), the coefficients of $\mathbf{x}(k)$ and $\mathbf{y}_{pd}^j(k)$ in Eq. (16) vanish simultaneously except for the ith uncertain sensor

$$\bar{\mathbf{C}}_s\bar{\mathbf{A}}^p + \bar{\mathbf{C}}_s\mathbf{M}_i\mathbf{O} = \mathbf{0}$$

$$\bar{\mathbf{C}}_s\boldsymbol{\tau}_j + \bar{\mathbf{C}}_s\mathbf{M}_i\mathbf{T}_j = \mathbf{0} \quad \text{for } j \neq i \tag{17}$$

Eq. (17) can be rewritten as

$$\begin{aligned} &\bar{\mathbf{C}}_s\mathbf{M}_i[\mathbf{T}_1 \ \cdots \ \mathbf{T}_{i-1} \ \mathbf{O} \ \mathbf{T}_{i+1} \ \cdots \ \mathbf{T}_{n_d}] \\ &\quad = -[\bar{\mathbf{C}}_s\boldsymbol{\tau}_1 \ \cdots \ \bar{\mathbf{C}}_s\boldsymbol{\tau}_{i-1} \ \bar{\mathbf{C}}_s\mathbf{A}^p \ \bar{\mathbf{C}}_s\boldsymbol{\tau}_{i+1} \ \cdots \ \bar{\mathbf{C}}_s\boldsymbol{\tau}_{n_d}] \end{aligned} \tag{18}$$

There are pn_s^2 unknown variables in $\bar{\mathbf{C}}_s\mathbf{M}_i$ and there are totally $n_s(p-1)(n_d-1)+n_sn$ equations in Eq. (18). A necessary condition for the existence of $\mathbf{CM}_i$ that satisfies Eq. (18) is

$$p(n_s - n_d + 1) \geqslant n - n_d + 1 \tag{19}$$

Satisfying Eq. (19) requires $n_s - n_d + 1 > 0$, which means that the number of independent reference sensors must be larger than or equal to the number of independent uncertain sensors. Also p must be larger than $(n-n_d+1)/(n_s-n_d+1)$. The product $\bar{\mathbf{C}}_s\mathbf{M}_i$ that satisfied Eq. (17) is not unique. But the $\bar{\mathbf{C}}_s\mathbf{M}_i$ solved from Eq. (18) using the pseudoinverse method produces a minimum-norm solution. Normally, p is selected to be several times larger than the required number that satisfies Eq. (19) to get a good numerical result.

Substituting the constraint condition in Eq. (17) into Eq. (16)

$$\begin{aligned} \mathbf{y}_s(k+p) &= (\bar{\mathbf{C}}_s\boldsymbol{\tau}_i + \bar{\mathbf{C}}_s\mathbf{M}_i\mathbf{T}_i)\mathbf{y}_{pd}^i(k) - \bar{\mathbf{C}}_s\mathbf{M}_i\mathbf{y}_{ps}(k) \\ &\quad + \sum_{j=1}^{r} \bar{\mathbf{C}}_s\bar{\mathbf{B}}_j\mathbf{y}_d^j(k+p-1) \end{aligned} \tag{20}$$

Up to this point, there still exist other uncertain sensor outputs $\mathbf{y}_d^j$ that contribute to the response $\mathbf{y}_s(k+p)$. $\mathbf{y}_d^j$ can be eliminated by premultiplying Eq. (20) with a row vector that is orthogonal to all remaining column vectors $\bar{\mathbf{C}}_s\bar{\mathbf{B}}_j$, $j \neq i$

$$\mathbf{N}_i^T(\bar{\mathbf{C}}_s\bar{\mathbf{B}}_j) = 0 \quad \text{for } \forall j \neq i \tag{21}$$

Since $n_s \geqslant n_r$, such a vector $\mathbf{N}_i^T$ can be easily found. Premultiplying Eq. (20) with $\mathbf{N}_i^T$ produces a scalar equation that involves measurements from all reference sensors and outputs from the ith examined uncertain sensor

$$\mathbf{N}_i^T\mathbf{y}_s(k+p) = \mathbf{N}_i^T(\bar{\mathbf{C}}_s\boldsymbol{\tau}_i + \bar{\mathbf{C}}_s\mathbf{M}_i\mathbf{T}_i)\mathbf{y}_{pd}^i(k) - \mathbf{N}_i^T\bar{\mathbf{C}}_s\mathbf{M}_i\mathbf{y}_{ps}(k) + \mathbf{N}_i^T\bar{\mathbf{C}}_s\bar{\mathbf{B}}_i\mathbf{y}_d^i(k+p-1) \tag{22}$$

In Eq. (22), the outputs from other uncertain sensors have been eliminated except for the monitored ith uncertain sensor. If $\bar{\mathbf{y}}_d^i(k)$ represents the measurement from the ith uncertain sensor at kth steps and $\mathbf{y}_d^{*i}(k)$ is the measurement error of the ith sensor at kth step, then $\mathbf{y}_d^i(k)=\bar{\mathbf{y}}_d^i(k)-\mathbf{y}_d^{*i}(k)$. Substituting $\mathbf{y}_d^i(k)=\bar{\mathbf{y}}_d^i(k)-\mathbf{y}_d^{*i}(k)$ into Eq. (22)

$$\mathbf{N}_i^T\mathbf{y}_s(k+p) = \mathbf{N}_i^T(\bar{\mathbf{C}}_s\boldsymbol{\tau}_i + \bar{\mathbf{C}}_s\mathbf{M}_i\mathbf{T}_i)(\bar{\mathbf{y}}_{pd}^i(k) - \mathbf{y}_{pd}^{*i}(k)) - \mathbf{N}_i^T\bar{\mathbf{C}}_s\mathbf{M}_i\mathbf{y}_{ps}(k) + \mathbf{N}_i^T\bar{\mathbf{C}}_s\bar{\mathbf{B}}_i(\bar{\mathbf{y}}_d^i(k+p-1) - \mathbf{y}_d^{*i}(k+p-1)) \tag{23}$$

By defining

$$e_i(k+p) = -\mathbf{N}_i^T(\bar{\mathbf{C}}_s\boldsymbol{\tau}_i + \bar{\mathbf{C}}_s\mathbf{M}_i\mathbf{T}_i)\mathbf{y}_{pd}^{*i}(k) - \mathbf{N}_i^T\bar{\mathbf{C}}_s\bar{\mathbf{B}}_i\mathbf{y}_d^{*i}(k+p-1) \tag{24}$$

Eq. (23) becomes

$$e_i(k+p) = \bar{\mathbf{N}}_i^T\mathbf{y}_s(k+p) + \bar{\mathbf{N}}_i^T\bar{\mathbf{C}}_s\bar{\mathbf{M}}_i\mathbf{y}_{ps}(k) - \bar{\mathbf{N}}_i^T(\bar{\mathbf{C}}_s\boldsymbol{\tau}_i + \bar{\mathbf{C}}_s\mathbf{M}_i\mathbf{T}_i)\bar{\mathbf{y}}_{pd}^i(k) - \mathbf{N}_i^T\bar{\mathbf{C}}_s\bar{\mathbf{B}}_i\bar{\mathbf{y}}_d^i(k+p-1) \tag{25}$$

Failure of the ith uncertain sensor can be detected and isolated by the error function in Eq. (25). When there are no measurement errors for the ith uncertain sensor from k to $k+p$ steps, $e_i(k+p)$ is zero. When there are measurement errors from step k to step $k+p$, the error function $e_i(k+p)$ will normally be different from zero. In the above procedure, there are two conditions that need to be satisfied for the error function to be valid: (1) $n_d \geqslant r$ to ensure the pseudoinverse of $\mathbf{D}_d$ to exist uniquely; and (2) $n_s \geqslant n_d$ to ensure $\bar{\mathbf{C}}_s\mathbf{M}_i$ exists.

Sensor Error Function Computed Directly from Input–Output Data

An alternative way to calculate the sensor error function directly from the measurement data instead of state-space matrices $\bar{\mathbf{A}}$, $\bar{\mathbf{B}}$, $\bar{\mathbf{C}}_s$ is introduced next. The following definitions are used to simplify the equations in Eq. (25) at the kth-th step: $\boldsymbol{\alpha}_i=[-\mathbf{N}_i^T(\bar{\mathbf{C}}_s\boldsymbol{\tau}_i+\bar{\mathbf{C}}_s\mathbf{M}_i\mathbf{T}_i), -\mathbf{N}_i^T\bar{\mathbf{C}}_s\bar{\mathbf{B}}_i]$, $\boldsymbol{\beta}_i=[\mathbf{N}_i^T\bar{\mathbf{C}}_s\mathbf{M}_i, \mathbf{N}_i^T]$, $\mathbf{y}_{ms}(k)=[\mathbf{y}_{ps}(k-p), \mathbf{y}_s(k)]^T$, and $\mathbf{u}_{ms}^i(k)=[\bar{\mathbf{y}}_{pd}^i(k-p), \bar{y}_d^i(k-1)]^T$. The error equation in Eq. (25) can be simplified as

$$e_i(k) = [\boldsymbol{\beta}_i, \boldsymbol{\alpha}_i]\begin{bmatrix}\mathbf{u}_{ms}^i(k)\\ \mathbf{y}_{ms}(k)\end{bmatrix} \tag{26}$$

If there is no measurement error for the ith uncertain sensor from the $(k\text{-}p)$th step to the kth step, the error equation in Eq. (26) is zero, regardless of the working status of other uncertain sensors. So the coefficients $[\boldsymbol{\beta}_i, \boldsymbol{\alpha}_i]$ satisfy

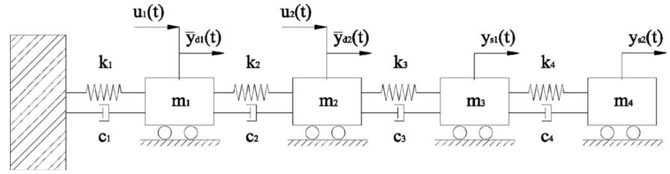

Fig. 1. Four degree-of-freedom spring-mass-damper system

$$0 = [\boldsymbol{\beta}_i, \boldsymbol{\alpha}_i]\begin{bmatrix}\mathbf{u}_{ms}^i(k)\\ \mathbf{y}_{ms}(k)\end{bmatrix} \tag{27}$$

Express Eq. (27) for l steps

$$\mathbf{0} = [\boldsymbol{\beta}_i, \boldsymbol{\alpha}_i]\mathbf{W}_{NY}^i$$

$$\mathbf{W}_{NY}^i = \begin{bmatrix}\mathbf{u}_{ms}^i(k) & \mathbf{u}_{ms}^i(k+1) & \cdots & \mathbf{u}_{ms}^i(k+l-1) & \mathbf{u}_{ms}^i(k+l)\\ \mathbf{y}_{ms}(k) & \mathbf{y}_{ms}(k+1) & \cdots & \mathbf{y}_{ms}(k+l-1) & \mathbf{y}_{ms}(k+l)\end{bmatrix} \tag{28}$$

Applying singular value decomposition (SVD) for $\mathbf{W}_{NY}^i$

$$\mathbf{W}_{NY}^i = [\mathbf{U}_1, \mathbf{U}_2]\begin{bmatrix}\mathbf{S}_1 & \mathbf{0}\\ \mathbf{0} & \mathbf{0}\end{bmatrix}\begin{bmatrix}\mathbf{V}_1^T\\ \mathbf{V}_2^T\end{bmatrix} \tag{29}$$

In order for Eq. (28) to be satisfied, $[\boldsymbol{\beta}_i, \boldsymbol{\alpha}_i]$ must belong to $\mathbf{U}_2$ (which is the left nullspace of $\mathbf{W}_{NY}^i$). Hence $[\boldsymbol{\beta}_i, \boldsymbol{\alpha}_i]$ is not unique. For a noise free case, any vector that belongs to the left nullspace of $\mathbf{W}_{NY}^i$ can be used as $[\boldsymbol{\beta}_i, \boldsymbol{\alpha}_i]$ in Eq. (26) to calculate the error function. If there are measurement noises in the uncertain sensors, the vector corresponding to the minimum singular value can be taken as $[\boldsymbol{\beta}_i, \boldsymbol{\alpha}_i]$. This is consistent with the $[\boldsymbol{\beta}_i, \boldsymbol{\alpha}_i]$ calculated from system statespace matrices $\bar{\mathbf{A}}$, $\bar{\mathbf{B}}$, $\bar{\mathbf{C}}_s$. The general solution for Eq. (18) is a subspace, which normally has an infinite number of $\bar{\mathbf{C}}_s\mathbf{M}_i$ that satisfy Eq. (18). Using pseudoinverse to calculate $\bar{\mathbf{C}}_s\mathbf{M}_i$ produces a minimum-norm solution. It is worth emphasizing here that coefficients $[\boldsymbol{\beta}_i, \boldsymbol{\alpha}_i]$ calculated directly from healthy measurement data are different from the coefficients $[\boldsymbol{\beta}_i, \boldsymbol{\alpha}_i]$ calculated from the system state-space matrix. But both coefficients vector $[\boldsymbol{\beta}_i, \boldsymbol{\alpha}_i]$ have the same function: the sensor error function calculated from both $[\boldsymbol{\beta}_i, \boldsymbol{\alpha}_i]$ will be nonzeros only if the corresponding uncertain sensor fails to correctly measure the structural responses and it will not be influenced by the measurement of the other uncertain sensors. Also to obtain the coefficients of sensor failure detection function, the measured data from the healthy state of the system should contain the frequency range that the structure spans. So band-limited white noise input is used to excite the structure and l needs to be taken large enough such that the time segment of the data used to build the coefficient of sensor error function is at least several times larger than the fundamental period of the structure. Unlike the inverse model (Kammer 1997, Kammer and Steltzner 2001), in which the initial condition is assumed to be zero, the sensor failure detection formulation has already systematically eliminated the initial conditions.

Simulation

A four degree-of-freedom (DOF) spring-mass-damper system is first used to testify the sensor failure detection algorithms, as shown in Fig. 1. Four accelerometer sensors are attached from

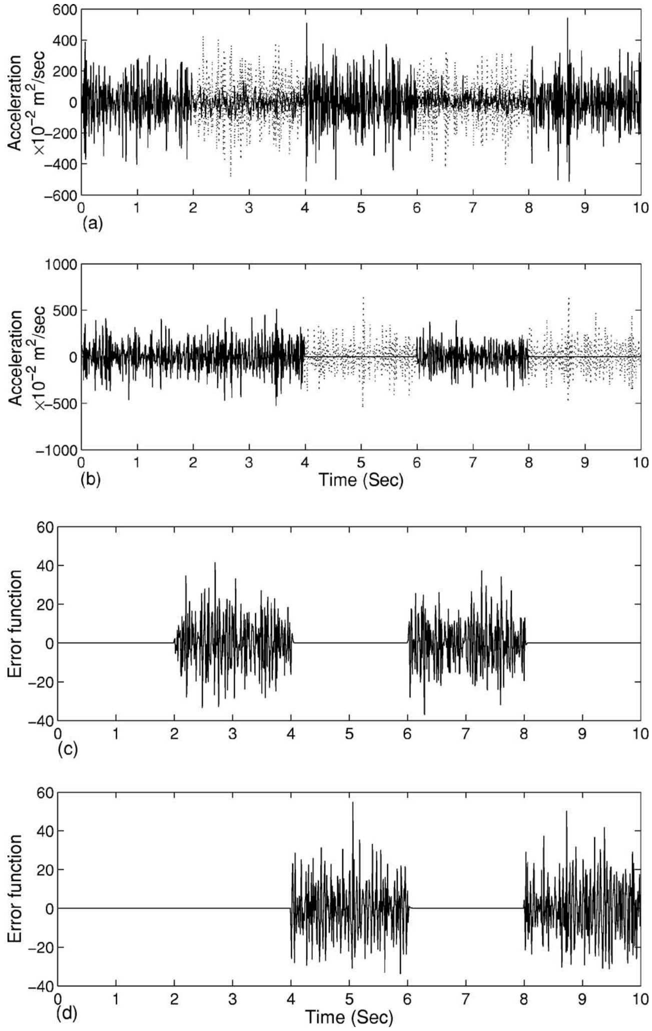

Fig. 2. Structural responses and error functions of Sensors 1 and 2 with coefficients $[\boldsymbol{\beta}_i, \boldsymbol{\alpha}_i]$ calculated from system state-space matrix using indirect approach for noise free case: (a) Sensor 1 (… structural responses, —sensor output); (b) Sensor 2 (…structural response, — sensor output); (c) error function of Sensor 1; and (d) error function of Sensor 2

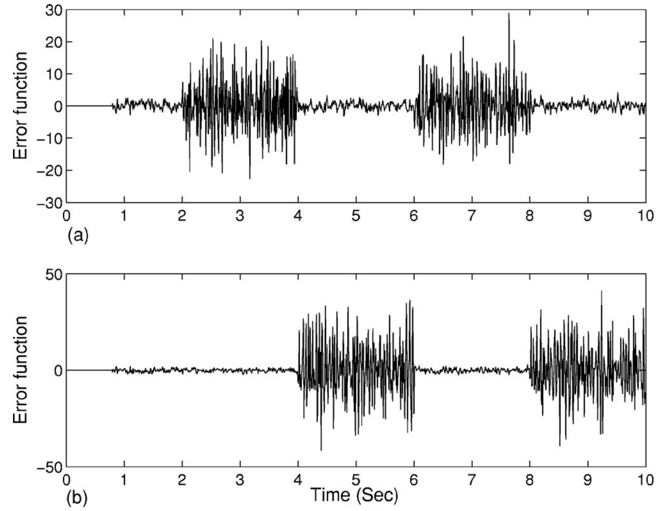

Fig. 3. Error functions of Sensor 1 and Senor 2 with coefficients $[\boldsymbol{\beta}_i, \boldsymbol{\alpha}_i]$ calculated from system state-space matrix using indirect approach for 1% standard deviation measurement noises in sensors on Mass 3 and 4: (a) error function of sensor 1; (b) error function of sensor 2

m_1 to m_4 and those sensors are separated into two groups. The first two sensors attached to m_1 and m_2 are assumed to be uncertain sensors. The other two sensors attached to m_3 and m_4 are assumed to be reference sensors. Note that since the input has been eliminated from the sensor error function and only the measurements from the reference sensors and uncertain sensors are required to build the sensor error function, as shown in Eq. (25), for this system, $m_1 = m_2 = m_3 = m_4 = 1$ kg, $k_1 = k_2 = k_3 = k_4 = 100$ kN/m, and $c_i = 0.05m_i + 0.001k_i$ N sec/m. Actuators 1 (u_1) and 2 (u_2) are driven by independent band-limited white noise input. In order to simulate sensor failure, the measurements from sensors attached to m_1 (Sensor 1) are set to arbitrary random data instead of actual structural responses during 2–4 and 6–8 s and the sensor attached to m_2 (Sensor 2) reads uniform zero measurements during 4–6 and 8–10 s. The structural responses and sensor measurements are shown in Figs. 2(a and b). The error functions of Sensors 1 and 2 for the noise free case are shown in Figs. 2(c and d). From Figs. 2(c and d) it is clear that the sensor error functions produce nonzero error signal when measurement errors occur. Otherwise, the error function shows zero values. Also each sensor error function uniquely indicates the corresponding sensor's failure and it is not influenced by the other uncertain sensors. Fig. 3 shows the sensor error functions with 1% standard deviation noise-corrupted data from all reference sensors. It can be seen that the error function can still identify the instant failure of each sensor. It is noted that the corruption of measurement noise on reference sensors will make the error functions nonzero even when the corresponding uncertain sensor correctly measures the structural response. However, in the current simulation, the amplitude of the error function produced by the measurement noise is much less than that of the failure case.

The sensor error function described above is based on the analytical model of the spring-mass-damper system. If the analytical model of the system is not known and only test data are available, the error function can be directly calculated by the procedure described from Eqs. (26)–(29). First, a data set from healthy sensors (both reference sensors and the examined uncertain sensor) is needed to calculate the coefficients $[\boldsymbol{\beta}_i, \boldsymbol{\alpha}_i]$ for subsequent computation of sensor error function. Then, the sensor error function can be used to indicate whether there are measurement errors in the uncertain sensor examined. Fig. 4(a) shows the sensor error functions for the noise free case and Fig. 4(b) shows the sensor error functions for the 1% standard deviation noise (on all reference sensors) case computed using the direct approach. It shows that the sensor error functions can successfully detect and isolate the examined uncertain sensor failure in real-time.

Experiment

The NASA eight-bay truss structure at Rice University, shown in Fig. 5, is used to verify the aforementioned sensor failure detection algorithm. The eight bay truss consists of 36 nodes and 109 aluminum members. The truss members are made up of hollow tubes fitted with aluminum bolt ends that can be screwed into the nodes. One end of the truss is mounted to a steel frame, which is fixed to the ground. The total truss length is 4 m. Two hangers are

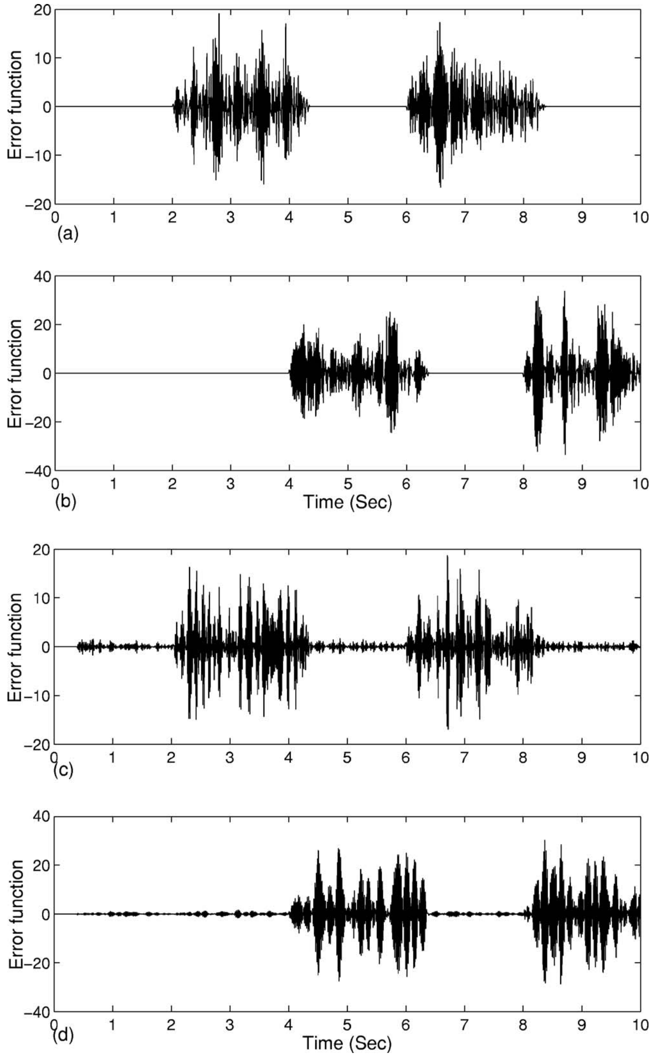

Fig. 4. Error functions of Sensor 1 and 2 with coefficients $[\boldsymbol{\beta}_i, \boldsymbol{\alpha}_i]$ calculated from healthy measurement data using direct approach: (a) error function of Sensor 1 (noise free case); (b) error function of Sensor 2 (noise free case); (c) error function of Sensor 1 (1% noise case); and (d) error function of Sensor 2 (1% noise case)

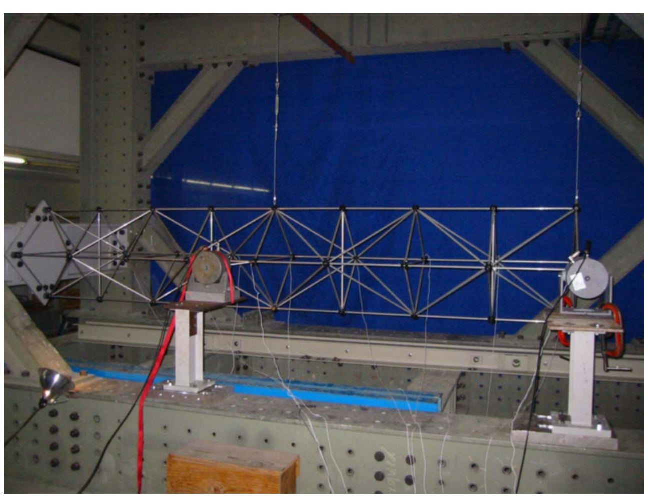

Fig. 5. Four-meter-long NASA eight-bay truss structure

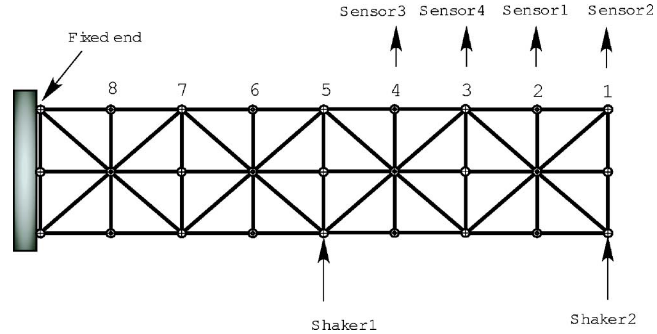

Fig. 6. Schematic of 4 long NASA eight-bay truss structure (plan view)

vertically connected to the truss node at the fourth and eighth bays (counted from the fixed end) to restrain vertical movement, as shown in Fig. 5. The experimentally identified fundamental frequency of the truss is 12.45 Hz (fundamental period of 0.08 s). Two electromagnetic shakers are attached to the first and fourth bay of the truss structure by stingers to produce horizontal excitation. Load cells are installed between the shaker stingers and the nodes of the truss to measure the actual input forces. Four accelerometers are mounted on the nodes of the truss from the first to the fourth bay to measure the horizontal responses of the truss at those nodes, as shown in Fig. 6. For this experiment, the accelerometers mounted on the third and fourth bays are assumed to be the reference sensors that correctly measure the structural responses. These reference sensors are used to monitor the conditions of uncertain accelerometer sensors on the first and second bays.

The two shakers, excited by band limited white noise generated by two amplifiers, are controlled by a 1102 DSpace board. Load cells and accelerometers are first connected to PCB a 481A signal conditioner and then connected to the DSpace board, attached to a computer. The sampling time is 0.001 s and the input-output data are recorded up to 80 s. The sensor on the first bay (Sensor 2) was disconnected from the signal conditioner from

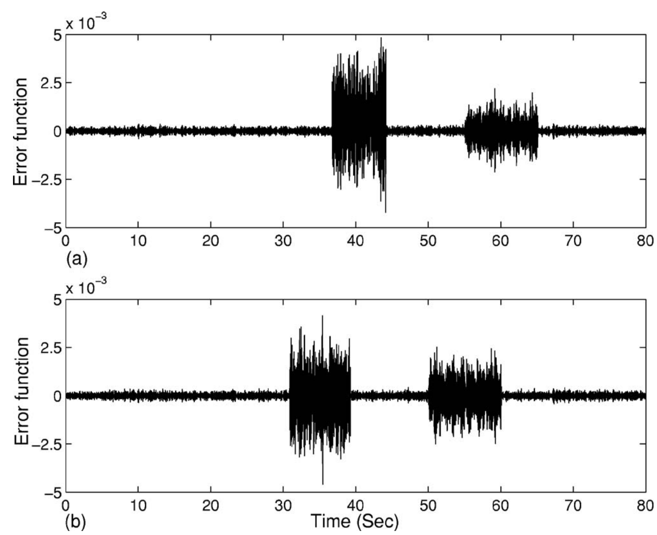

Fig. 7. Experimental sensor error functions of Sensor 1 and Sensor 2 of NASA eight-bay truss structure with coefficients $[\boldsymbol{\beta}_i, \boldsymbol{\alpha}_i]$ obtained from healthy measurement data using direct approach: (a) error function of Sensor 1; (b) error function of Sensor 2

31 to 39 s to simulate one type of sensor failure in which the sensor fails to measure the structural response and produces no measurement. Between 50 and 60 s the amplitude of the output from Sensor 2 was reduced by half using a built in function in the Simulink toolbox to simulate an amplitude reduction type of sensor failure. The sensor on the second bay (Sensor 1) was disconnected from the signal conditioner from 36.5 to 44 s and the amplitude of outputs was reduced by 40% from 55 to 65 s. The first 1.5 s of data, which is nearly 19 times the fundamental period of the truss structure, was used to generate coefficients $[\boldsymbol{\beta}_i, \boldsymbol{\alpha}_i]$ by the procedure described from Eqs. (26)–(29) and the error function was computed using the coefficients. In this experiment, $p=150$ and $l=1{,}500$ (l-data length) were adopted.

The experimentally determined sensor error functions using the direct approach, for Sensors 1 and 2, are shown in Fig. 7. Each sensor error function can uniquely detect and isolate the instant failure of the corresponding uncertain sensor, regardless of the condition of the other uncertain sensors. From Fig. 7, it can also be observed that the amplitude profiles of the sensor error function corresponding to the zero output failure case are larger than that of the amplitude reduction case. There are small nonzero values in the error function even when the sensors are functioning correctly, which is primarily due to measurement noise in the reference sensors. However, there is one order of magnitude difference between sensor failure and error due to measurement noise. In the experiment, the maximum amplitude of the measurement noises of those accelerometers is around $0.02\ \mathrm{m/s^2}$. The maximum amplitude of the structural responses excited by shakers is around $0.4\ \mathrm{m/s^2}$. So the amplitudes of the measurement noises are around 5% of that of the structural responses.

Conclusion

A new sensor failure detection method has been presented to monitor the instant of sensor failure. The error function is based on the interaction matrix formulation between reference and uncertain sensors. Input has been eliminated from sensor error functions in this formulation. Two new approaches have been presented in this paper. In the first approach the sensor error function is computed indirectly from the state-space model by combining the inverse model with the interaction matrix formulation to eliminate the input and all uncertain sensor terms except for the examined one from the sensor error functions. In the second approach, the coefficients of the sensor error functions are directly computed from the null space of the healthy measurement data using the singular value decomposition method. The applicability of the sensor failure detection formulation has been demonstrated both numerically by a four degree-of-freedom spring-mass-damper system and experimentally by a 4 m long eight bay truss structure. The error function clearly detects the instants of failure of the uncertain sensors in the presence of reasonable experimental measurement noise.

Acknowledgments

The writers wish to acknowledge the support of the Texas Institute for the Intelligent Bio-Nano Materials and Structure for Aerospace Vehicles, funded by NASA Cooperative Agreement No. NCC-1-02038.

References

Beard, R. V. (1971), "Fault accommodation in linear systems through self-reorganization." *Rep. Man-Vehicle Laboratory MVT-71-1*, MIT, Cambridge, Mass.

Chen, R., and Speyer, J. L. (2001), "Fault reconstruction from sensor and actuator failures." *Proc., 40th IEEE Conf. on Decision and Control*, Orlando, Fla., 2227–2282.

Da, R., and Lin, C. F. (1995), "Sensor failure detection with a bank of kalman filters." *Proc., American Control Conf.*, Seattle, 1122–1126.

Dharap, P., Koh, B. H., and Nagarajaiah, S. (2006). "Structural health monitoring using ARMarkov observers." *J. Intell. Mater. Syst. Struct.*, 17(6), 469–481.

Frank, P. M. (1990). "Fault diagnosis in dynamic systems using analytical and knowledge-based redundancy—A survey and some new results." *Automatica*, 26(3), 459–474.

Gertler, J. (1991). "A survey of fault detection and identification methods." *Proc., IFAC, IMACS Safe Process Symp.*, Baden, Baden, Germany.

Goodzeit, N. E., and Phan, M. Q. (2000). "System identification in the presence of completely unknown periodic disturbances." *J. Guid. Control Dyn.*, 23(2), 251–259.

Jones, H. L. (1976). "Fault detection in linear systems." *The Charles Stark Draper Laboratory Rep. No. T-608*, Cambridge, Mass.

Kammer, D. C. (1997). "Estimation of structural response using remote sensor locations." *J. Guid. Control Dyn.*, 20(3), 501–508.

Kammer, D. C., and Steltzner, A. D. (2001). "Strucutral identification of Mir using inverse system dynamics and Mir/shuttle docking data." *J. Vibr. Acoust.*, 123(2), 230–237.

Koh, B. H., Dharap, P., Nagarajaiah, S., and Phan, M. Q. (2005a). "Real-time structural damage monitoring by input error function." *AIAA J.*, 43(8), 1808–1814.

Koh, B. H., Li, Z., Dharap, P., Nagarajaiah, S., and Phan, M. Q. (2005b). "Actuator failure detection through interaction matrix formulation." *J. Guid. Control Dyn.*, 28(5), 895–901.

Lim, R. K., Phan, M. Q., and Longman, R. W. (1998). "State estimation with ARMarkov models." *Department of Mechanical and Aerospace Eng. Tech. Rep. No. 3046*, Princeton Univ., N.J.

Menke, T. E. (1995). "Sensor/actuator failure detection in the Vista F-16 by multiple model adaptive estimation." *IEEE Trans. Aerosp. Electron. Syst.*, 31(4), 1218–1229.

Park, J. H., Rizzoni, G., and Ribbons, W. B. (1993). "On the representation of sensor faults in fault detection filters." *Proc., 32nd Conf. on Decision and Control*, San Antonio, 1728–1732.

Phan, M. Q., Lim, R. K., and Longman, R. W. (1998). "Unifying input-output and state-space perspective of predictive control." *Department of Mechanical and Aerospace Engineering Technical Rep. No. 3044*, Princeton Univ., N.J.

Piercy, N. P. (1992). "Sensor failure estimators for detection filters." *IEEE Transactions Automatic Detection Filters*, 37(10), 1553–1558.

Steltzner, A. D., and Kammer, D. C. (1999). "Input force estimation using an inverse structural filter." *Proc., 17th Int. Modal Analysis Conf.*, SEM, Kissimmee, Fla., 954–960.